Synthesis, Characterization, and Electrochemistry of Heteroleptic Double-Decker Complexes of the Type Phthalocyaninato−Porphyrinato−Zirconium(IV) or −Hafnium(IV)

Roger Guilard,*[1a] Jean-Michel Barbe,[1a] Amina Ibnlfassi,[1b] Abdallah Zrineh,[1b,d] Victor A. Adamian,[1c] and Karl M. Kadish*[1c]

LIMSAG (UMR 9953) and Laboratoire de Synthèse et d'Electrosynthèse Organométalliques (UMR 1685), Faculté des Sciences "Gabriel", Université de Bourgogne, 6 Boulevard Gabriel, 21100 Dijon, France, and Department of Chemistry, University of Houston, Houston, Texas 77204-5641

Received September 7, 1994[⊗]

The synthesis, spectroscopic characterization, and electrochemistry of 12 different neutral, singly and doubly oxidized heteroleptic double-decker complexes of the type $[M^{IV}(P)(Pc)]^n$ where n = 0, +1, or +2, M = Zr or Hf, P = the dianion of octaethylporphyrin (OEP) or tetraphenylporphyrin (TPP), and Pc = the dianion of phthalocyanine are reported. Each neutral compound was characterized by ^{1}H NMR, UV−visible, and IR spectroscopy while each oxidized or reduced compound was characterized by UV−visible and/or EPR spectroscopy. The neutral compounds all undergo two reversible ring-centered oxidations and two reversible ring-centered reductions. Comparison is made with data obtained for the corresponding actinide double-decker complexes containing Th(IV) or U(IV) central metal ions and correlations examined between $E_{1/2}$ for all of the compounds and either the metal ionic radius or the absorbance band energy of the porphyrin Soret or phthalocyanine UV−band. The half-wave potentials depend upon the type of macrocycle. They also vary with the size of metal ion in the case of oxidation but not in reduction, where $E_{1/2}$ values are relatively unaffected and shift by only 20−40 mV upon going from Hf(P)(Pc) to Th(P)(Pc) as compared to a much larger 220−280 mV shift between $E_{1/2}$ for the first oxidation of the same compounds.

Introduction

Synthetic double-decker compounds can be divided into two groups, those which have the same macrocycle (called homoleptic complexes) and those which have different macrocycles (called heteroleptic complexes). Homoleptic bis(phthalocyanines) have been synthesized and characterized with titanium,[2] tin,[3,4] zirconium,[5,6] hafnium,[5] uranium,[7−9] and thorium[7−9] metal ions as well as with most lanthanide metal ions.[10−14] Bis(porphyrin) complexes containing two identical[15−27,30] or two different macrocycles[27−32] have also been synthesized with the same metal ions except for titanium and tin. This contrasts with the heteroleptic complexes containing one porphyrin and one phthalocyanine macrocycle which, to date, have only been reported for the case of Ce(IV),[33] U(IV),[30] and Th(IV)[30] derivatives. These unsymmetrical double-decker compounds

[⊗] Abstract published in *Advance ACS Abstracts,* February 15, 1995.

(1) (a) Université de Bourgogne (UMR 9953). (b) Université de Bourgogne (URA 1685). (c) University of Houston. (d) On leave from the Laboratoire de Chimie Physique Générale, Département de Chimie, Faculté des Sciences, Université Mohammed V, Rabat, Morocco.
(2) Ercolani, C.; Paoletti, A. M.; Pennesi, G.; Rossi, G.; Chiesi-Villa, A.; Rizzoli, C. *J. Chem. Soc., Dalton Trans.* **1990,** 1971−1977.
(3) Kroenke, W. J.; Kenney, M. E. *Inorg. Chem.* **1964,** *3,* 251−254.
(4) Bennett, W. E.; Broberg, D. E.; Baenziger, N. C. *Inorg. Chem.* **1973,** *12,* 930−936.
(5) Tomilova, L. G.; Ovchinnikova, N. A.; Luk'yanets, E. A. *Zh. Obshch. Khim.* **1987,** *57,* 2100−2104 (*Russ. J. Chem., (Engl. Transl.)* **1988,** 1880−1883).
(6) Silver, J.; Lukes, P. J.; Howe, S. D.; Howlin, B. *J. Mater. Chem.* **1991,** *1,* 29−35.
(7) Lux, F.; Dempf, D.; Graw, D. *Angew. Chem., Int. Ed. Engl.* **1968,** *7,* 919−920.
(8) Lux, F.; Ammentorp-Schmidt, F.; Dempf, D.; Graw, D.; Hasenberg, W. *Radiochim. Acta* **1970,** *14,* 57−61.
(9) Gieren, A.; Hoppe, W. *J. Chem. Soc., Chem. Commun.* **1971,** 413−414.
(10) De Cian, A.; Moussavi, M.; Fischer, J.; Weiss, R. *Inorg. Chem.* **1985,** *24,* 3162−3167.
(11) Moussavi, M.; De Cian, A.; Fischer, J.; Weiss, R. *Inorg. Chem.* **1988,** *27,* 1287−1291.
(12) Konami, H.; Hatano, M.; Tajiri, A. *Chem. Phys. Lett.* **1989,** *160,* 163−167.
(13) Konami, H.; Hatano, M.; Kobayashi, N.; Osa, T. *Chem. Phys. Lett.* **1990,** *165,* 397−400.
(14) Pondaven, A.; Cozien, Y.; L'Her, M. *New J. Chem.* **1992,** *16,* 711−718.
(15) Buchler, J. W.; Kapellmann, H. G.; Knoff, M.; Lay, K.-L.; Pfeifer, S. *Z. Naturforsch* **1983,** *38B,* 1339−1345.
(16) Buchler, J. W.; De Cian, A.; Fischer, J.; Kihn-Botulinski, M.; Paulus, H.; Weiss, R. *J. Am. Chem. Soc.* **1986,** *108,* 3652−3659.
(17) Buchler, J. W.; Elsässer, K.; Kihn-Botulinski, M.; Scharbert, B. *Angew. Chem., Int. Ed. Engl.* **1986,** *25,* 286−287.
(18) Kim, K.; Lee, W. S.; Kim, H. J.; Cho, S. H.; Girolami, G. S.; Gorlin, P. A.; Suslick, K. S. *Inorg. Chem.* **1991,** *30,* 2652−2656.
(19) Buchler, J. W.; De Cian, A.; Fischer, J.; Hammerschmitt, P.; Weiss, R. *Chem. Ber.* **1991,** *124,* 1051−1058.
(20) Kim, H. J.; Whang, D.; Kim, J.; Kim, K. *Inorg. Chem.* **1992,** *31,* 3882−3886.
(21) Buchler, J. W.; De Cian, A.; Elschner, S.; Fischer, J.; Hammerschmitt, P.; Weiss, R. *Chem. Ber.* **1992,** *125,* 107−115.
(22) Buchler, J. W.; Eberle, M.; Hammerschmitt, P.; Huttermann, J.; Kappl, R. *Chem. Ber.* **1993,** *126,* 2619−2623.
(23) Buchler, J. W.; Hüttermann, J.; Löffler, J. *Bull. Chem. Soc. Jpn.* **1988,** *61,* 71−77.
(24) Girolami, G. S.; Milam, S. N.; Suslick, K. S. *J. Am. Chem. Soc.* **1988,** *110,* 2011−2012.
(25) Buchler, J. W.; Kihn-Botulinski, M.; Scharbert, B. *Z. Naturforsch.* **1988,** *43B,* 1371−1380.
(26) (a) Buchler, J. W.; Hammerschmitt, P.; Kaufeld, I.; Löffler, J. *Chem. Ber.* **1991,** *124,* 2151−2159. (b) Buchler, J. W.; Kihn-Botulinski, M.; Löffler, J.; Scharbert, B. *New J Chem* **1992,** *16,* 545−553.
(27) Girolami, G. S.; Gorlin, P. A.; Milam, S. N.; Suslick, K. S.; Wilson, S. R. *J. Coord. Chem.* **1994,** *32,* 173−212.
(28) Radzki, S.; Mack, J.; Stillman, M. J. *New. J. Chem.* **1992,** *16,* 583−589.
(29) (a) Buchler, J. W.; De Cian, A.; Fischer, J.; Hammerschmitt, P.; Löffler, J.; Scharbert, B.; Weiss, R. *Chem. Ber.* **1989,** *122,* 2219−2228. (b) Buchler, J. W.; Löffler, J. *Z. Naturforsch.* **1990,** *45B,* 531−542.
(30) Kadish, K. M.; Moninot, G.; Hu, Y.; Dubois, D.; Ibnlfassi, A.; Barbe, J.-M.; Guilard, R. *J. Am. Chem. Soc.* **1993,** *115,* 8153−8166.
(31) Bilsel, O.; Rodriguez, J.; Milam, S. N.; Gorlin, P. A.; Girolami, G. S.; Suslick, K. S.; Holten, D. *J. Am. Chem. Soc.* **1992,** *114,* 6528−6538.
(32) Girolami, G. S.; Gorlin, P. A.; Suslick, K. S. *Inorg. Chem.* **1994,** *33,* 626−627.

0020-1669/95/1334-1472$09.00/0

Table 1. ^{1}H NMR Data (δ, in ppm vs TMS) for M(P)(Pc) Complexes in $CDCl_3$ at 25 °C[a]

metal	macrocycles		Pc resonances		TPP resonances				OEP resonances		
			H_α	H_β	pyr H	*o*-H	*m*-H	*p*-H	meso H	$-CH_2-$	$-CH_3$
Hf	OEP	Pc	9.16 (br)	8.15 (br)					9.16 (br)	3.80 (br)	1.66 (t)
Zr			9.17 (br)	8.16 (br)					9.17 (br)	3.81 (m)	1.67 (t)
Hf	TPP	Pc	9.21 (br)	8.24 (br)	8.31 (s)	7.67 (m) 6.11 (d)	7.19 (d) 7.05 (m)	7.54 (t)			
Zr			9.20 (br)	8.22 (br)	8.29 (s)	7.67 (m) 6.14 (d)	7.18 (d) 7.06 (m)	7.54 (t)			

[a] Key: dd = double doublet, s = singlet, d = doublet, t = triplet, br = broad signal, m = multiplet.

can be oxidized or reduced by up to four electrons, with the main site of electron transfer being assigned in many cases to either the porphyrin or the phthalocyanine macrocycle, depending upon the specific compound and specific redox reaction.[30] In contrast, a localized site of electron transfer on one of the two macrocycles is not seen upon oxidation or reduction of the symmetrical double-decker compounds.[34]

Double-decker porphyrins and phthalocyanines can be considered as good model compounds for studying $\pi-\pi$ interactions that occur between two macrocycles located in close proximity to each other. It is well-known that such interactions play an important role in natural systems, particularly in the photosynthetic "special pair".[35] Previously studied double-decker porphyrins and phthalocyanines have included derivatives with rather large metal ions, *i.e.*, those with ionic radii of 0.98–1.16 Å for the trivalent metals in the lanthanide series, 1.00 Å for U(IV), and 1.05 Å for Th(IV).[36] It has been shown that the distance between two macrocycles of a given synthetic double-decker compound is related to the redox potentials and other physical properties of these compounds, and in order to study this in more detail, we have now synthesized and characterized new heteroleptic porphyrin and phthalocyanine derivatives with the smaller Zr(IV) and Hf(IV) metal ions having ionic radii of 0.84 and 0.83 Å, respectively. The symmetrical bis(phthalocyanine) and bis(porphyrin) complexes of Zr and Hf are well characterized in the literature,[5,6,18–22] but only a single report exists on the unsymmetrical bis(porphyrin) Zr complex.[32]

In the present paper we report the synthesis, electrochemistry, and spectroscopic (UV-vis, IR, ^{1}H NMR, and EPR) characterization of eight heteroleptic double-decker compounds having the general formula $[M^{IV}(P)(Pc)]^{n+}$ where $n = 0$, 1, or 2, M = Zr or Hf, P = the dianion of octaethylporphyrin (OEP) or tetraphenylporphyrin (TPP), and Pc = the dianion of phthalocyanine. A comparison is made between the spectroscopic and electrochemical properties of these compounds and the related heteroleptic double-decker derivatives containing either a U(IV) or a Th(IV) metal ion.

Experimental Section

Instrumentation. All electrochemical measurements were carried out using a conventional three-electrode system. A glassy carbon disk of approximately 0.07 cm^2 surface area served as the working electrode, and a platinum wire was used as the counter electrode. The reference electrode was a homemade saturated calomel electrode (SCE) which was separated from the working solution by a fritted glass bridge.

Cyclic voltammetry was performed with an IBM EC 225 2A voltammetric analyzer or an EG&G Princeton Applied Research (PAR) Model 173 potentiostat coupled to an EG&G Model 175 universal programmer. Current–voltage curves were recorded on an EG&G Model RE 0151 X-Y recorder. Thin-layer spectroelectrochemical measurements were made with an EG&G Model 173 potentiostat coupled with a Princeton Instruments ST-1000 controller and PDA-1024 diode array. OSMA and PSMA softwares were used for data acquisition and processing with IBM PC386 computer. The design of the thin-layer cell is described elsewhere.[37]

UV–visible spectra were obtained with an IBM 9430 or a Varian Cary I spectrophotometer. Infrared spectra of solid samples were obtained as a 1% dispersion in CsI using a Nicolet 205 or a Bruker IFS 66 V FTIR spectrophotometer. *In-situ* Fourier transform infrared (FTIR) measurements were carried out with a homemade IR-transparent spectroelectrochemical cell using an IBM IR 32 spectrometer which was coupled with an IBM 9000 computer system and an EG&G Model 173 potentiostat.

EPR spectra were recorded on a Bruker Model ER 100D spectrometer equipped with an ER 040-X microwave bridge and an ER 080 power supply. The g values were measured relative to diphenylpicrylhydrazyl (DPPH) ($g = 2.0037 \pm 0.0002$). The spectrometer was equipped with a variable-temperature apparatus, and an Omega Model DR-41 RTD digital thermocouple was inserted into the cavity to monitor changes of temperature.

^{1}H NMR spectra were recorded on a Bruker WM 400 spectrometer of the "Centre de Spectrométrie Moléculaire" at the Université de Bourgogne. Spectra were measured in 0.5 mL of C_6D_6 using tetramethylsilane as a reference.

Mass spectra were obtained using a Kratos Concept 32 S of the "Centre de Spectrométrie Moléculaire" at the Université de Bourgogne in the positive DCI mode (desorption chemical ionization) with NH_3 as a reactant gas.

Materials. Dichloromethane (CH_2Cl_2) was purchased from Fluka and used as received. Tetra-*n*-butylammonium perchlorate, TBAP, purchased from Kodak, recrystallized from absolute ethanol, and then dried and stored in a vacuum oven at 40 °C. All syntheses were performed under an argon atmosphere using Schlenk techniques.

(Octaethylporphyrinato)(phthalocyaninato)zirconium(IV), Zr(OEP)(Pc). $Na_2(Pc)$ was used as the starting reactant in the synthesis and was prepared according to a previously described procedure.[38] Zr(OEP)Cl_2 was synthesized using the method described by Brand and Arnold[39] with the slight modifications given below.

$(OEP)H_2$ (0.4 g) was dissolved in 1,2-dimethoxyethane (80 mL), after which 1.5 mL of 1 M of $LiN(Si(CH_3)_3)_2$ (1.5 mmol) in hexane was added to the solution. The mixture was stirred until the color turned bright red (~15 min). The subsequent addition of 1.2 *g* of $ZrCl_4(THF)_2$ (3.18 mmol) followed by refluxing for 2 h led to the formation of Zr(OEP)Cl_2. After filtration and evaporation of the solvent, 1 *g* of Na_2(Pc) (1.8 mmol) and 50 mL of 1-chloronaphthalene were introduced into the flask and the solution was refluxed for 3 h, with the progress of the reaction being monitored by UV–visible spectroscopy. Evaporation of the solvent and column chromatography (SiO_2, 30 × 5 cm column) of the crude solid with toluene as eluent gave H_2(OEP) as the first fraction, Zr(OEP)(Pc) as the second fraction, and finally the singly-oxidized species as the third and final fraction. Neutral Zr(OEP)(Pc)

(33) Lachkar, M.; De Cian, A.; Fischer, J.; Weiss, R. *New. J. Chem.* **1988**, *12*, 729–731.
(34) (a) Duchowski, J. K.; Bocian, D. F. *J. Am. Chem. Soc.* **1990**, *112*, 3312–3318. (b) Duchowski, J. K.; Bocian, D. F. *Inorg. Chem.* **1990**, *29*, 4158–4160.
(35) Deisenhofer, J.; Epp, O.; Miki, K.; Huber, R.; Michel, H. *J. Mol. Biol.* **1984**, 385–398.
(36) Shannon, R. D. *Acta Crystallogr., Sect. A* **1976**, *32*, 751–767.
(37) Lin, X. Q.; Kadish, K. M. *Anal. Chem.* **1985**, *57*, 1498–1501.
(38) Barrett, P. A.; Dent, C. E.; Linstead, R. P. *J. Chem. Soc.* **1936**, 1719–1736.
(39) Brand, H.; Arnold, J. *J. Am. Chem. Soc.* **1992**, *114*, 2266–2267.

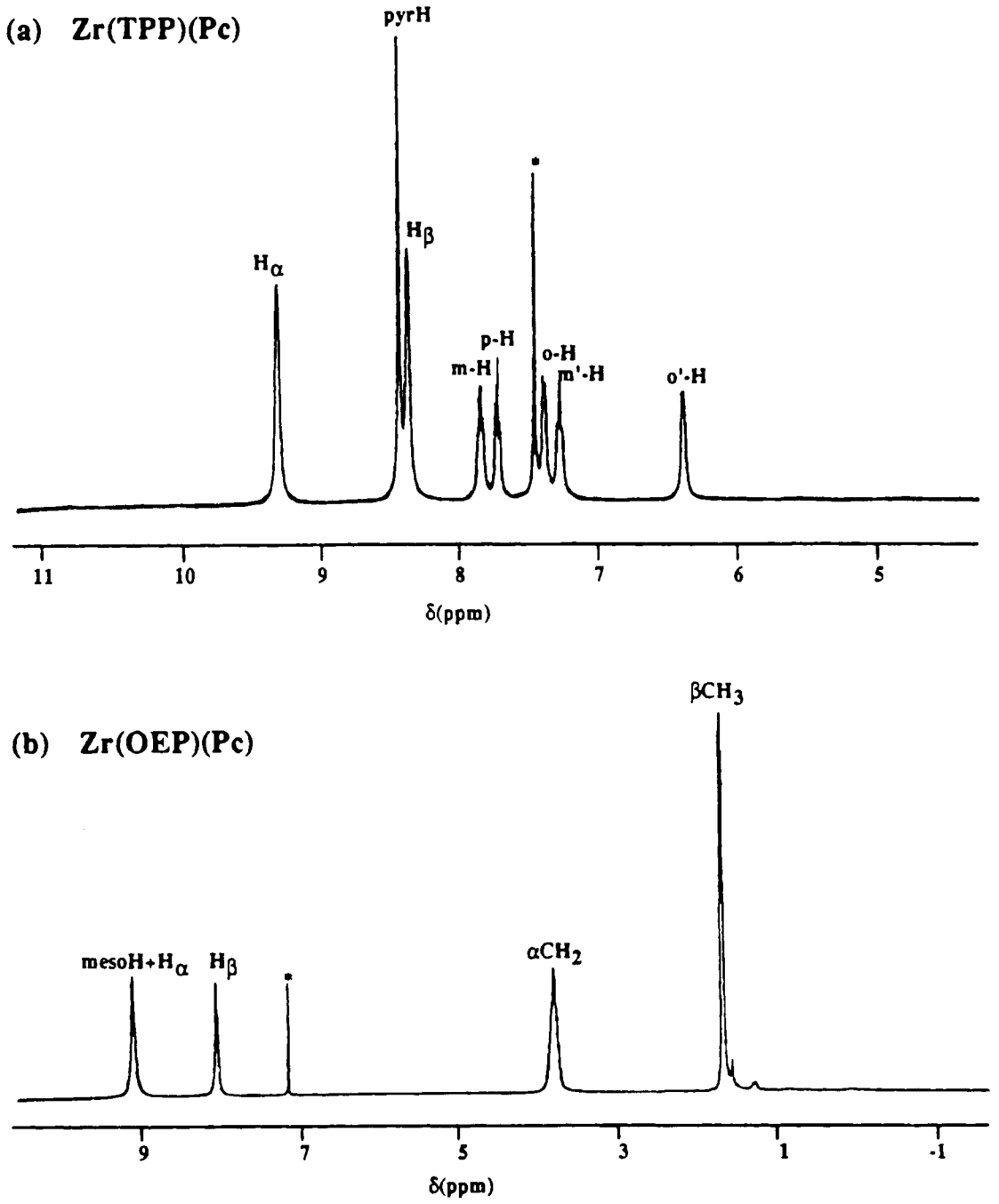

Figure 1. ^{1}H NMR spectra of (a) Zr(TPP)(Pc) and (b) Zr(OEP)(Pc) in $CDCl_3$ at 298 K. (∗ = nondeuterated solvent).

was recovered from this last fraction by addition of excess hydrazine hydrate. Heptane was added to the Zr(OEP)(Pc) fraction in order to facilitate precipitation, and after evaporation of most of the solvent, 0.45 *g* (69%) of Zr(OEP)(Pc) were obtained. MS (*m/z* assignment, % abundance): 1135 $(M + H)^+$, 100.

Syntheses of the other investigated compounds given below follow the above described method.

(Tetraphenylporphyrinato)(phthalocyaninato)zirconium(IV), Zr(TPP)(Pc). A 0.5 *g* sample of $(TPP)H_2$ (0.81 mmol), 2 mL of a 1 M solution of $LiN(Si(CH_3)_3)_2$ (2 mmol) in hexane, 1.2 *g* of $ZrCl_4(THF)_2$ (3.22 mmol), and 1.0 *g* of $Na_2(Pc)$ (1.8 mmol) gave 0.25 *g* (25%) of Zr(TPP)(Pc) after recrystallization from a 1:1 dichloromethane/heptane mixture. MS (*m/z* assignment, % abundance): 1215 $(M + H)^+$, 100.

(Octaethylporphyrinato)(phthalocyaninato)hafnium(IV), Hf(OEP)(Pc). A 0.22 *g* sample of $(OEP)H_2$ (0.81 mmol), 1 mL of a 1 M solution of $LiN(Si(CH_3)_3)_2$ (1 mmol) in hexane, 0.6 *g* of $HfCl_4(THF)_2$ (1.29 mmol), and 0.4 *g* of $Na_2(Pc)$ (0.72 mmol) gave 0.16 *g* (32%) of Hf(OEP)(Pc) after recrystallization from a 1:1 toluene/heptane mixture. MS ((m/z assignment, % abundance): 1225 $(M + H)^+$, 100.

(Tetraphenylporphyrinato)(phthalocyaninato)hafnium(IV), Hf(TPP)(Pc). A 0.2 *g* amount of $(TPP)H_2$ (0.33 mmol), 0.7 mL of a 1 M solution of $LiN(Si(CH_3)_3)_2$ (0.7 mmol) in hexane, 0.48 *g* of $HfCl_4(THF)_2$ (1.03 mmol), and 0.4 *g* of $Na_2(Pc)$ (0.72 mmol) gave 0.15 *g* (35%) of Hf(TPP)(Pc) after recrystallization from a 1:1 dichloromethane/heptane mixture. MS (*m/z* assignment, % abundance): 1305 $(M + H)^+$, 100.

Oxidized Species. A reaction of the neutral compounds with 1 or 2 equiv of the phenoxathiinylium radical in dichloromethane[30] gave the singly- and doubly-oxidized compounds as described below. The same procedure was used for all the oxidized species and is detailed for $[Zr(OEP)(Pc)][SbCl_6]$ and $[Zr(OEP)(Pc)][SbCl_6]_2$.

(Octaethylporphyrinato)(phthalocyaninato)zirconium(IV) Hexachloroantimonate, [Zr(OEP)(Pc)][SbCl$_6$]. To a solution of 0.05 *g* of Zr(OEP)(Pc) (0.044 mmol) in 7 mL of CH_2Cl_2 was added 0.024 *g* of [phenoxathiine][$SbCl_6$] radical (0.046 mmol) in 4 mL of CH_2Cl_2. The subsequent addition of 10 mL of heptane to the reaction mixture led to the crystallization of $[Zr(OEP)(Pc)][SbCl_6]$. A 0.05 *g* quantity (77% yield) of this complex was collected after filtration.

Table 2. UV−Visible and NIR Data for [M(P)(Pc)]^n Complexes in CH_2Cl_2 Where n = 0, +1, or +2[a]

metal	macrocycles		n	λ, (nm) ($10^{-4}\epsilon$, dm^3 mol^{-1} cm^{-1}) Pc	Soret	Q″		Q′		near-IR
Zr	TPP	Pc	0	340 (6.55)	400 (6.91)	457 (3.54)	468 (3.47)	579 (1.76)	600 (2.78)	
			+1	341 (6.78)	383 (6.89)	469 (4.81)		582 (1.36)		752 (0.92), 1010 (br)
			+2	330 (sh)	371 (4.65)	473 (3.47)				858 (br)
	OEP	Pc	0	342 (10.84)	383 (9.86)	450 (2.79)		549 (2.67)	644 (4.44)	
			+1	340 (4.21)	~365 (sh)	455 (1.71)		518 (sh)	602 (1.13)	766 (0.51), 1070 (br)
			+2	345 (4.13)		440 (1.67)			631 (0.95)	782 (3.37, br)
Hf	TPP	Pc	0	336 (6.19)	398 (6.85)	457 (3.60)	466 (3.51)	578 (1.72)	660 (2.26)	
			+1	342 (7.13)	382 (7.26)	468 (5.13)		584 (1.42)		754 (0.96), 1000 (br)
			+2	331 (sh)	369 (5.15)	471 (4.11)				842 (br)
	OEP	Pc	0	339 (10.48)	381 (8.82)	447 (2.95)		553 (2.63)	646 (3.87)	
			+1	341 (4.90)	~365 (sh)	453 (1.77)		516 (sh)	601 (1.51)	768 (0.67), 1065 (br)
			+2	343 (4.84)		438 (1.21)			633 (0.93)	773 (3.49, br)

[a] Abbreviations: sh = shoulder; br = broad.

Table 3. Diagnostic Infrared Bands (cm^{-1}) of [M(P)(Pc)][$SbCl_6$] and [M(P)(Pc)][$SbCl_6$]$_2$ in KBr

metal	macrocycles		singly oxidized P band	singly oxidized Pc band	doubly oxidized P bands	doubly oxidized Pc band
Zr	OEP	Pc	1547	1319	1531, 1560	1315
Hf	OEP	Pc	1540	1321	1532, 1564	1316
Zr	TPP	Pc	1461	1319	1261, 1536, 1463	1316
Hf	TPP	Pc	1462	1321	1262, 1540, 1464	1314

(Tetraphenylporphyrinato)(phthalocyaninato)zirconium(IV) Hexachloroantimonate, [Zr(TPP)(Pc)][$SbCl_6$]. A 0.05 *g* sample of Zr(TPP)(Pc) (0.041 mmol) and 0.022 *g* of phenoxathiinylium radical (0.042 mmol) gave 0.038 *g* of [Zr(TPP)(Pc)][$SbCl_6$] (60% yield).

(Octaethylporphyrinato)(phthalocyaninato)hafnium(IV) Hexachloroantimonate, [Hf(OEP)(Pc)][$SbCl_6$]. A 0.02 *g* quantity of Hf(OEP)(Pc) (0.016 mmol) and 0.009 *g* of phenoxathiinylium radical (0.016 mmol) gave 0.022 *g* of [Hf(OEP)(Pc)][$SbCl_6$] (88% yield).

(Tetraphenylporphyrinato)(phthalocyaninato)hafnium(IV) Hexachloroantimonate, [Hf(TPP)(Pc)][$SbCl_6$]. A 0.04 *g* sample of Hf(TPP)(Pc) (0.031 mmol) and 0.017 *g* of phenoxathiinylium radical (0.031 mmol) gave 0.04 *g* of [Hf(TPP)(Pc)][$SbCl_6$] (79% yield).

(Octaethylporphyrinato)(phthalocyaninato)zirconium(IV) Bis(hexachloroantimonate), [Zr(OEP)(Pc)][$SbCl_6$]$_2$. A solution of 0.03 *g* of Zr(OEP)(Pc) (0.026 mmol) and 0.03 *g* of [phenoxathiine][$SbCl_6$] radical (0.056 mmol) in 10 mL of CH_2Cl_2 was stirred for 2 h. The addition of 10 mL of heptane gave after filtration 0.03 *g* (64% yield) of a crystalline powder of [Zr(OEP)(Pc)][$SbCl_6$]$_2$.

(Tetraphenylporphyrinato)(phthalocyaninato)zirconium(IV) Bis(hexachloroantimonate), [Zr(TPP)(Pc)][$SbCl_6$]$_2$. A 0.03 *g* quantity of Zr(TPP)(Pc) (0.025 mmol) and 0.03 *g* of phenoxathiinylium radical (0.056 mmol) gave 0.035 *g* of [Zr(TPP)(Pc)][$SbCl_6$]$_2$ (74% yield).

(Octaethylporphyrinato)(phthalocyaninato)hafnium(IV) Bis(hexachloroantimonate), [Hf(OEP)(Pc)][$SbCl_6$]$_2$. A 0.03 *g* quantity of Hf(OEP)(Pc) (0.025 mmol) and 0.028 *g* of phenoxathiinylium radical (0.052 mmol) gave 0.02 *g* of [Hf(OEP)(Pc)][$SbCl_6$]$_2$ (42% yield).

(Tetraphenylporphyrinato)(phthalocyaninato)hafnium(IV) Bis(hexachloroantimonate), [Hf(TPP)(Pc)][$SbCl_6$]$_2$. A 0.024 *g* quantity of Hf(TPP)(Pc) (0.018 mmol) and 0.022 *g* of phenoxathiinylium radical (0.041 mmol) gave 0.03 *g* of [Hf(TPP)(Pc)][$SbCl_6$]$_2$ (85% yield).

Results and Discussion

Synthesis. The M(P)(Pc) complexes were synthesized according to eq 1 using a previously reported method.[30]

$$M(P)Cl_2 \xrightarrow[\text{reflux, 2 h}]{Na_2(Pc),\ \text{chloronaphthalene}} M(P)(Pc) \qquad (1)$$

M = Zr or Hf; P = OEP or TPP

The starting M(P)Cl_2 derivatives were obtained from Li_2(P)(DME)$_n$ (DME = 1,2-dimethoxyethane) and $MCl_4(THF)_2$ using literature methods.[39] A reaction of the dichlorometal(IV) porphyrin with Na_2(Pc) then gave the desired M(P)(Pc) derivatives in yields ranging from 25 to 69%. Trace amounts of free base porphyrin and bis(phthalocyanine) metal complexes were also obtained. The M(P)(Pc) derivatives are easily oxidized and some of the singly-oxidized species were also detected during purification by column chromatography.

Table 4. EPR Parameters for [M(P)(Pc)][$SbCl_6$]

compound	central line g[a]	central line ΔH,[b] G	zero-field splitting D, cm^{-1} × 10^4 298 K, solid state	zero-field splitting D, cm^{-1} × 10^4 110 K, frozen soln[c]
[Hf(TPP)(Pc)][$SbCl_6$]	2.002	3.2	no triplet comp	35
[Zr(TPP)(Pc)][$SbCl_6$]	2.002	3.2	no triplet comp	35
[Hf(OEP)(Pc)][$SbCl_6$]	2.002	4.1	45	34
[Zr(OEP)(Pc)][$SbCl_6$]	2.002	3.9	49	34

[a] Solid state, 298 K. [b] In the solid state. ΔH = 5.4 G for [Zr(OEP)(Pc)]$^{+\cdot}$ and 6.26 G for [Zr(TPP)(Pc)]$^{+\cdot}$ in a 10^{-3} M solution in CH_2Cl_2 at 298 K. [c] 10^{-3} M in CH_2Cl_2.

^{1}H NMR Spectra of the Neutral Complexes. The ^{1}H NMR spectra of the zirconium and hafnium double-decker derivatives are similar to each other and show features typical of complexes with diamagnetic metal centers. A summary of the NMR data is given in Table 1, and the spectra of Zr(OEP)(Pc) and Zr(TPP)(Pc) are shown in Figure 1. The meso proton resonances of the OEP unit in Zr(OEP)(Pc) appear at 9.17 ppm and are overlapped with resonances from the H_α protons of the Pc ring. There is also a triplet at 1.67 ppm (α-CH_2) and a broad resonance at 3.81 ppm (β-CH_3). The two different proton sites of the phthalocyanine ring exhibit resonances at 9.17 (H_α protons) and 8.16 ppm (H_β protons).

The phenyl groups of the TPP moiety in Zr(TPP)(Pc) show five signals, as expected for such a double-decker complex,[30] and these are located at 7.67 and 6.14 (*o*-H), 7.18 and 7.06 (*m*-H), and 7.54 ppm (*p*-H). The pyrrole protons appear as a singlet at 8.29 ppm whereas resonances from the H_α and H_β protons of the phthalocyanine macrocycle are located at 9.20 and 8.22 ppm, respectively. The same pattern is observed for the Hf(P)(Pc) complexes.

UV−Visible Spectra. The heteroleptic M(P)(Pc) derivatives possess two major bands in the UV region of the spectrum. One is located at 336−342 nm and the other at 381−400 nm. This contrasts with the homoleptic derivatives, which have a single UV band located at ~340 nm for M(Pc)$_2$[5] and ~380 nm for M(P)$_2$.[18,19] A comparison of spectroscopic data for the homoleptic and heteroleptic complexes having the same metal

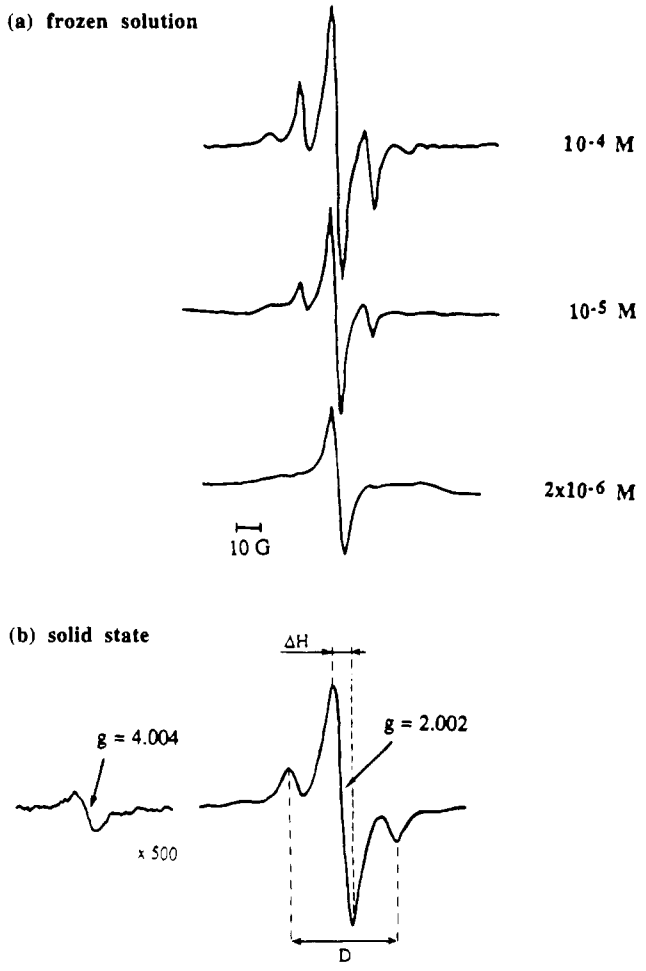

Figure 2. EPR spectra of $[Zr(OEP)(Pc)][SbCl_6]$ (a) at different concentrations in frozen CH_2Cl_2 at 110 K and (b) in the solid state at 298 K.

ions allows one to ascribe the more blue-shifted UV band of M(P)(Pc) (at 336−342 nm) to the Pc ring of the compound and the red-shifted one (at 381−400 nm) to the porphyrin ring. All of the neutral compounds also have an additional absorption located between 447 and 457 nm. This band, which has been attributed to transitions from delocalized orbitals involving both macrocycles, is labelled as Q′ in Table 2 and is characteristic of the double-decker complexes.[30,31]

Soret band absorptions of the M(P)(Pc) derivatives containing a Zr(IV) or Hf(IV) metal ion are all blue-shifted by ca. 15−20 nm when compared to those of the heteroleptic U(IV),[30] Th(IV),[30] and Ce(IV)[33] compounds with the same set of macrocycles. This shift is induced by the smaller ionic radius of the Hf(IV) and Zr(IV) metal ions, which leads to a shorter distance between the two macrocycles in these double-decker compounds. The UV−visible properties of the Hf and Zr heteroleptic complexes are also similar to each other (see Table 2).

The two $[M(TPP)(Pc)]^+$ derivatives exhibit separate UV−visible bands that can be associated with either the phthalocyanine or the porphyrin macrocycle of the complex. The porphyrin Soret band of $[M(TPP)(Pc)]^+$ is blue-shifted by 16−17 nm from the bands of the neutral complex and by another 12−13 nm upon going from $[M(TPP)(Pc)]^+$ to $[M(TPP)(Pc)]^{2+}$, *i.e.*, from 400 nm for the neutral Zr(TPP)(Pc) complex to 383 and 371 nm for the singly- and doubly-oxidized derivatives, respectively. The UV−visible spectra of $[M(OEP)(Pc)]^+$ are also characterized by separate porphyrin and phthalocyanine bands (see Table 2), but this is not the case for $[M(OEP)(Pc)]^{2+}$, where no discernible absorptions of the dication can be attributed to the porphyrin Soret band, which has either disappeared or blue-shifted such that it becomes overlapped with the Pc band which appears at 340−345 nm. The diagnostic Q″ absorption bands are again observed for the singly- and doubly-oxidized compounds, and these fall in the range 438−473 nm (see Table 2).

In addition, the singly- and doubly-oxidized derivatives are all characterized by diagnostic[40] bands in the near-IR region of the spectrum. These bands result from a transition between the split HOMO orbitals of the two macrocycles and appear at a wavelength whose position reflects the magnitude of the interaction.[34,35] A broad band is seen for the singly-oxidized $[M(TPP)(Pc)]^+$ derivatives at ~1010 nm (M = Zr) or 1000 nm (M = Hf), and a similar band is seen for $[M(OEP)(Pc)]^+$ at 1070 nm (M = Zr) or 1065 nm (M = Hf). The corresponding bands of the doubly-oxidized compounds are shifted to 858 nm (M = Zr) or 842 nm (M = Hf) for $[M(TPP)(Pc)]^{2+}$ and to 782 nm (M = Zr) or 773 nm (M = Hf) for $[M(OEP)(Pc)]^{2+}$. All of these absorptions are red-shifted by 80−100 nm with respect to corresponding bands of the bis(porphyrin) complexes,[20,21] thus indicating a diminished $\pi-\pi$ interaction in the oxidized heteroleptic species, as compared to the oxidized homoleptic ones.

IR Spectra. Monomeric porphyrin π-cation radicals generally exhibit a diagnostic infrared band which is located at 1250−1300 cm^{-1} for compounds with TPP macrocycles and at 1500−1600 cm^{-1} for those with OEP macrocycles.[41] These diagnostic bands are also seen for the singly-oxidized homoleptic compounds and are located at 1325 cm^{-1} for $[Zr(TPP)_2]^{\bullet+}$ and 1555 cm^{-1} for $[Zr(OEP)_2]^{\bullet+}$.[21] There is also an additional band at 1319 cm^{-1} which is present only in the spectra of the heteroleptic $[M(P)(Pc)]^+$ and $[M(P)(Pc)]^{2+}$ complexes (M = U or Th) and is apparently associated with the phthalocyanine π-cation radical.[30] A Pc marker band located at 1319 cm^{-1} is also seen in addition to an OEP marker band at 1547 cm^{-1} for $[Zr(OEP)(Pc)]^+$ (see Table 3). The observation of diagnostic bands belonging to both the OEP and the Pc macrocycles is consistent with the electron being abstracted from a mixed OEP and Pc orbital upon the first one-electron oxidation of M(OEP)(Pc). The FTIR spectrum of electrogenerated $[Zr(OEP)(Pc)]^+$ in CH_2Cl_2 also reveals a new band at 1550 cm^{-1}, and this suggests that the same radical species is generated either chemically or electrochemically from Zr(OEP)(Pc).

The second one-electron oxidation of M(OEP)(Pc) leads to a species which has intense infrared bands at 1531, 1560, and 1315 cm^{-1} (M = Zr) or 1532, 1564, and 1316 cm^{-1} (M = Hf). The first two IR bands of each compound can be attributed to the OEP π-cation radical of $[M(OEP)(Pc)]^{2+}$, while the third band at ca. 1315 cm^{-1} is associated with the Pc π-cation radical of the same compound.[30,40]

Diagnostic π-cation radical bands of metalloporphyrins with TPP macrocycles cannot be observed in solutions containing tetrabutylammonium perchlorate as supporting electrolyte since this salt absorbs in this region of the spectrum.[30] Therefore, only infrared bands of the chemically generated $[M(TPP)(Pc)][SbCl_6]$ derivatives are presented in this paper. The singly-oxidized compounds have intense broad bands at 1319 and 1461 cm^{-1} for $[Zr(TPP)(Pc)][SbCl_6]$ and at 1321 and 1462 cm^{-1} for $[Hf(TPP)(Pc)][SbCl_6]$ (see Table 3). The first band can be associated with the Pc π-cation radical but the second (at 1461−1462 cm^{-1}) cannot be definitely assigned to the TPP macrocycle.

(40) Buchler, J. W.; Scharbert, B. *J. Am. Chem. Soc.* **1988**, *110*, 4272−4276.
(41) Shimomura, E. T.; Phillippi, M. A.; Goff, H. M. *J. Am. Chem. Soc.* **1981**, *103*, 6778−6780.

Table 5. Half-Wave Potentials (V vs SCE) for Oxidation and Reduction of Hf, Zr, U, and Th Double-Deckers in CH_2Cl_2 (Details in Experimental Section)

macrocycles				oxidation			reduction				
		metal	ionic radius(Å),[a]	1st	2nd	Δ_1[b]	1st	2nd	Δ_2[b]	HOMO−LUMO gap, V	ref
TPP	Pc	Hf	0.83	0.44	0.97	0.53	−0.85	−1.31	0.46	1.29	t.w.
		Zr	0.84	0.45	0.97	0.52	−0.87	−1.31	0.44	1.32	t.w.
		U	1.00	0.63	1.16	0.53	−0.82	−1.27	0.45	1.45	30
		Th	1.05	0.66	1.22	0.56	−0.84	−1.27	0.43	1.50	30
OEP	Pc	Hf	0.83	0.22	0.77	0.55	−0.98	−1.42	0.44	1.20	t.w.
		Zr	0.84	0.22	0.78	0.56	−0.98	−1.42	0.44	1.20	t.w.
		U	1.00	0.44	0.96	0.52	−0.92	−1.36	0.44	1.36	30
		Th	1.05	0.50	1.02	0.52	−0.94	−1.38	0.44	1.44	30
TPP	TPP	Hf	0.83	0.54	0.99	0.45	−1.29	−1.65	0.36	1.83	19
		Zr	0.84	0.53	0.98	0.45	−1.31	−1.70	0.39	1.84	19
		U	1.00	0.71	1.10	0.39	−1.27	−1.57	0.30	1.98	30
		Th	1.05	0.79	1.13	0.34	−1.27	−1.55	0.28	2.06	30
OEP	OEP	Hf	0.83	−0.04	0.57	0.61	−1.66			1.62	19
		Zr	0.84	−0.03	0.57	0.60	−1.66			1.63	19
		U	1.00	0.23	0.79	0.56	−1.55			1.78	30
		Th	1.05	0.32	0.85	0.53	−1.53			1.85	30
Pc	Pc	Hf	0.83	0.48	1.02	0.54					5[c]
		Zr	0.84	0.54	1.08	0.54					5[c]
		U	1.00	0.74	1.09	0.35	−0.56	−0.87	0.31	1.30	30[d]
		Th	1.05	0.74	1.09	0.35	−0.57	−0.85	0.28	1.31	30[d]
Pc	L_2[g]	U	1.00	0.79			−0.83	−1.28	0.45	1.62	45[e]
		Th	1.05	0.73			−0.85	−1.29	0.44	1.58	45[e]
OEP	L_2[g]	U	1.00	0.58	1.26	0.68	−1.56			2.14	46[e]
		Th	1.05	0.76	1.15	0.39	−1.57	−1.98[f]	0.41	2.33	46[e]

[a] Ionic radii were taken from ref 36 for metal ions with coordination number 8. [b] Δ_1 = difference between $E_{1/2}$ of second and first oxidations, and Δ_2 = difference between $E_{1/2}$ of first and second reductions, respectively. [c] Measurements reported in 1,2-dichlorobenzene. [d] Measurements reported in pyridine. [e] Measurements reported in PhCN. [f] Irreversible process, E_{pc}. [g] L = acetylacetonate.

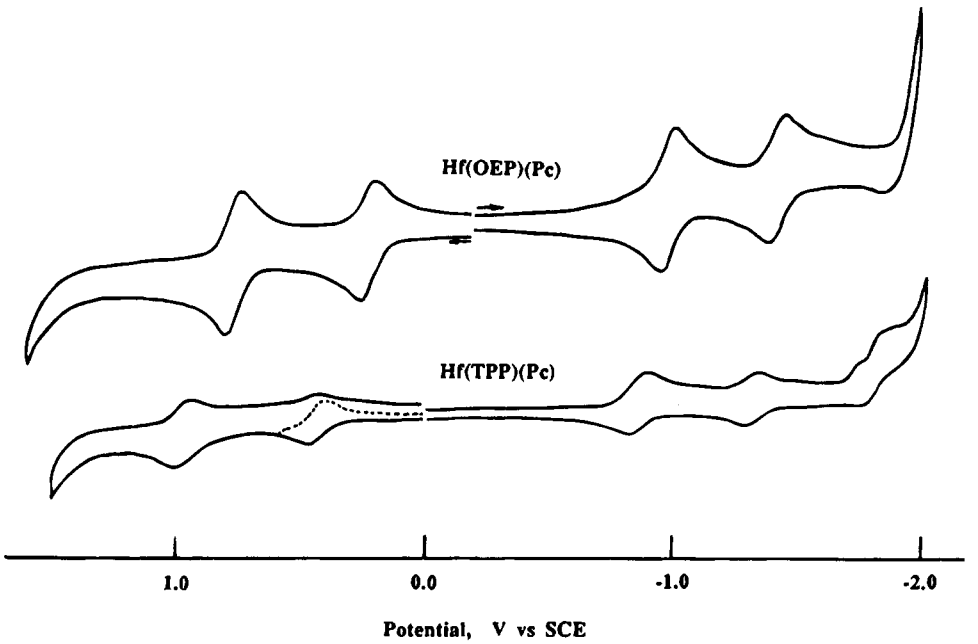

Figure 3. Cyclic voltammograms of Hf(OEP)(Pc) and Hf(TPP)(Pc) in CH_2Cl_2, 0.1 M TBAP. Scan rate = 0.1 V/s.

Infrared spectra of the doubly-oxidized $[M(TPP)(Pc)][SbCl_6]_2$ salts also show new absorptions at ~1261 and 1536−1540 cm^{-1} as well as a broad band at ~1315 cm^{-1}. The site of the unpaired electron in $[M(TPP)(Pc)]^{\bullet+}$ cannot be established on the basis of IR data alone, but this is not the case for $[M(TPP)(Pc)]^{2+}$, which has characteristic π-cation radical bands of both the TPP (~1261 cm^{-1}) and Pc (~1315 cm^{-1}) macrocycles, in agreement with the occurrence of a positive charge delocalization over both conjugated π ring systems.

EPR of Singly-Oxidized Compounds. Table 4 summarizes EPR data for $[M(P)(Pc)][SbCl_6]$ both in the solid state at 298 K and in CH_2Cl_2 solutions at 298 and 110 K. The compounds exhibit a typical metalloporphyrin π-cation radical signal at g = 2.002 under all three experimental conditions. The room-temperature line widths, ΔH, are between 3.2 and 4.1 G for the solid samples and between 5.4 and 6.2 G for the solutions.

EPR line widths of $[Zr(P)_2]^+$ have previously been used to determine the degree of electron delocalization in the radical.[22]

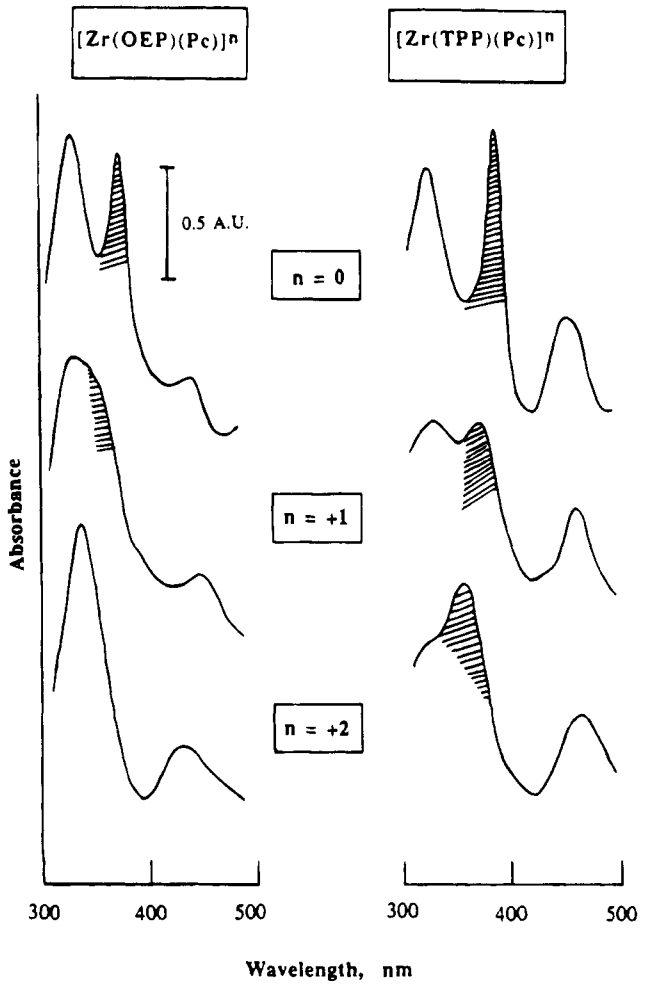

Figure 4. UV−visible spectra of neutral and electrooxidized Zr(OEP)(Pc) and Zr(TPP)(Pc) complexes in CH_2Cl_2, 0.1 M TBAP.

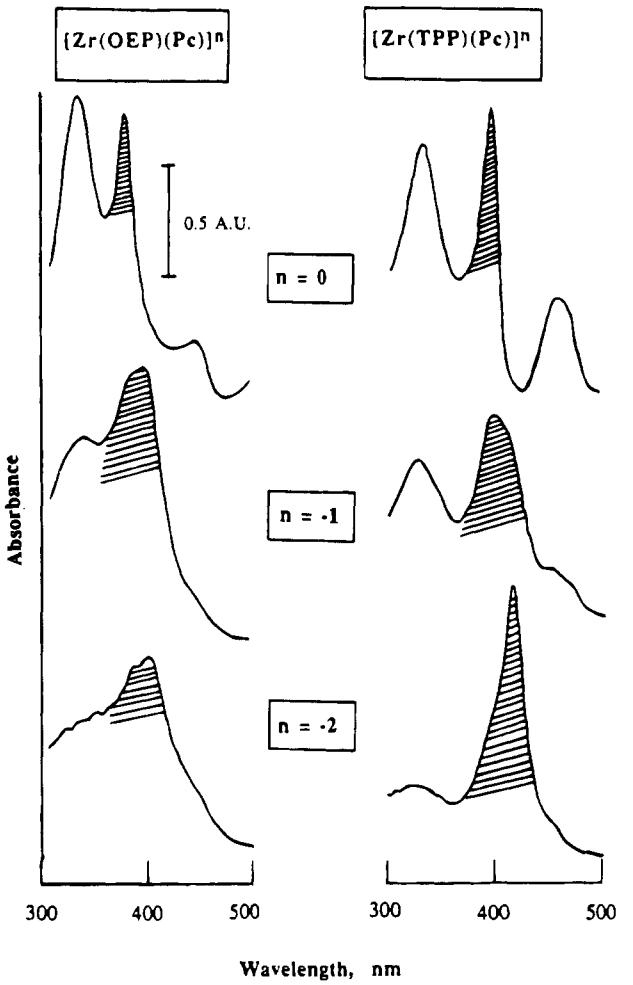

Figure 5. UV−visible spectra of neutral and electroreduced Zr(OEP)(Pc) and Zr(TPP)(Pc) complexes in CH_2Cl_2, 0.1 M TBAP.

Generally, double-decker porphyrin derivatives with a more localized unpaired electron density will show a broader EPR line with the maximum theoretical value of ΔH being $\sqrt{2}$ times larger when the electron is completely localized on one ring than when it is completely delocalized over the two rings. The values of ΔH are slightly higher for $[M(OEP)(Pc)]^{\bullet+}$ than for $[M(TPP)(Pc)]^{\bullet+}$, both in the solution and in the solid state (see Table 4), thus indicating that the unpaired electron on $[M(TPP)(Pc)]^{\bullet+}$ is more delocalized over the two macrocycles than in the case of the $[M(OEP)(Pc)]^{\bullet+}$.

The EPR spectra of $[Zr(P)(Pc)]^{\bullet+}$ and $[Hf(P)(Pc)]^{\bullet+}$ both show the presence of four lines in addition to the central one at 110 K in frozen CH_2Cl_2 solutions (see Figure 2a), and the overall shape of the spectrum is characteristic of a randomly-oriented solid in the triplet state.[42−44] This was previously observed for $[Th(P)(Pc)]^{\bullet+}$ under the same conditions and was explained by the formation of π-cation radical dimers having the general formula $[(^{\bullet+}Por)Th(Pc)\cdots(Pc)Th(Por^{\bullet+})]$, *i.e.*, a species with two unpaired electrons. $[Zr(OEP)(Pc)][SbCl_6]$ and $[Hf(OEP)(Pc)][SbCl_6]$ both show triplet signals at 298 K in the solid state, but this is not the case for $[Th(OEP)(Pc)][SbCl_6]$, for which only a simple π-cation radical signal is observed.[30] No triplet signals are seen for any of the $[M(TPP)(Pc)][SbCl_6]$ derivatives (M = Th,[30] Zr, or Hf) in the solid state, either at room temperature or at 110 K.

Triplet EPR signals can be definitively characterized[42−44] by a half-field absorption at $g \sim 4$, but this absorption is generally weak and could not be observed for frozen solutions of the singly-oxidized compounds (due to their low concentrations). However, a weak absorption was observed at $g = 4.004$ for both $[Zr(OEP)(Pc)][SbCl_6]$ and $[Hf(OEP)(Pc)][SbCl_6]$ in the solid state (Figure 2b).

The distance, r, between two unpaired electrons in the π-cation radical dimer of $[M(P)(Pc)]^{\bullet+}$ can be estimated from the zero-field splitting parameter, D, according to eq (2).[30,43]

$$r = (0.65g^2/D)^{1/3} \quad (2)$$

The value of D was found to be (45 to 49) $\times 10^{-4}$ cm^{-1} for $[M(OEP)(Pc)][SbCl_6]$ (Table 4) and this corresponds to an average 9 Å distance between two unpaired electrons in the solid state.

The relative intensity of the triplet vs the singlet component of the signal varies with the concentration of the compound in solution; *i.e.*, the higher the concentration, the higher is the intensity of the triplet component (see Figure 2a). The intensity of the signal absorption is proportional to the concentration of the radicals, and it was therefore possible to calculate an equilibrium constant, K, for the following monomer/dimer equilibrium:

$$M + M \rightleftarrows M_2 \quad (3a)$$

$$K = [M_2]/[M]^2 \quad (3b)$$

(42) Wasserman, E.; Snyder, L. C.; Yager, W. A. *J. Chem. Phys.* **1964**, *41*, 1763−1772.
(43) Lazarev, G. G. Z. *Phys. Chem.* **1991**, *173*, 141−165.
(44) Wertz, J. E.; Bolton, J. R. Electron Spin Resonance; McGraw Hill Book Co.: New York, 1972; p 230.

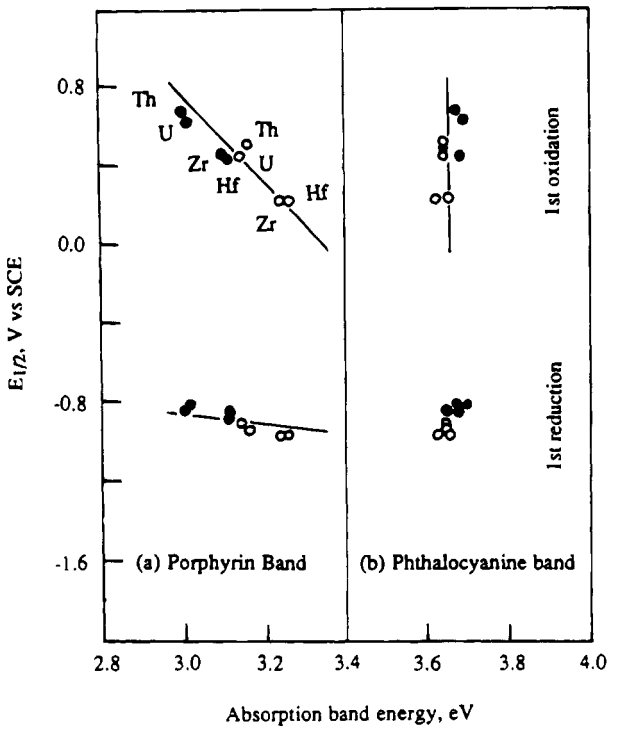

Figure 6. Correlations between $E_{1/2}$ for the first reduction or first oxidation of M(P)(Pc) and energies of (a) the porphyrin UV band and (b) the phthalocyanine UV band of the same compound. Compounds with the TPP macrocycle are represented by solid circles and those with the OEP macrocycle by open circles.

where M represents the monomeric π-cation radical and M_2 the π-cation radical dimer. The absorption intensities can be compared using eq 4[44] where Y is the peak-to-peak amplitude

$$I \sim Y(\Delta H)^2 \tag{4}$$

and ΔH the peak-to-peak separation of the first-derivative spectrum.

The use of eqs 3 and 4 gives an equilibrium constant of 10^7–10^8 M^{-1} for the four investigated compounds. An equilibrium constant of the same order of magnitude is also obtained from EPR data previously reported for singly-oxidized [Th(P)(Pc)]$^{\bullet+}$.[30] The relatively large equilibrium constant means that mainly dimeric species exist in frozen solutions at a compound concentration of 10^{-5}–10^{-3} M.

Electrochemistry and Spectroelectrochemistry. The first two oxidations and first two reductions of each investigated compound are reversible and involve a single electron transfer in CH_2Cl_2 containing 0.1 M TBAP as supporting electrolyte. The potentials for these reactions are summarized in Table 5, which also includes data from the literature on U and Th compounds. Two additional irreversible reductions are also observed for the M(TPP)(Pc) derivatives. These occur at E_{pc} = −1.73 and −1.85 V for M = Hf and at E_{pc} = −1.71 and −1.82 V for M = Zr. Representative cyclic voltammograms of Hf(TPP)(Pc) and Hf(OEP)(Pc) in CH_2Cl_2 are shown in Figure 3.

Each reversible redox reaction was monitored by spectroelectrochemistry in a thin-layer cell, and examples of the resulting UV−vis spectra for [Zr(OEP)(Pc)]^n and [Zr(TPP)(Pc)]^n after two subsequent oxidations (n = +1 or +2) or two subsequent reductions (n = −1 or −2) are shown in Figures 4 and 5. The two oxidations of M(OEP)(Pc) lead to a diminishing in intensity of the porphyrin Soret band, which also shifts toward the blue, but the Pc UV band remains almost unchanged. This contrasts with the M(TPP)(Pc) complexes, where the oxidation leads to a decrease in intensity for both the TPP and Pc absorption bands while the position of the TPP Soret band (shaded in Figure 4) blue-shifts and that of the Pc band remains relatively unchanged.

The stepwise one-electron reductions of M(OEP)(Pc) and M(TPP)(Pc) affect mainly the Pc band in the UV−vis spectra (see Figure 5), which decreases in intensity as the intensity of the porphyrin Soret band remains almost the same (P = OEP) or even increases (P = TPP). Finally, it should be noted that the diagnostic double-decker Q″ band of M(P)(Pc) disappears

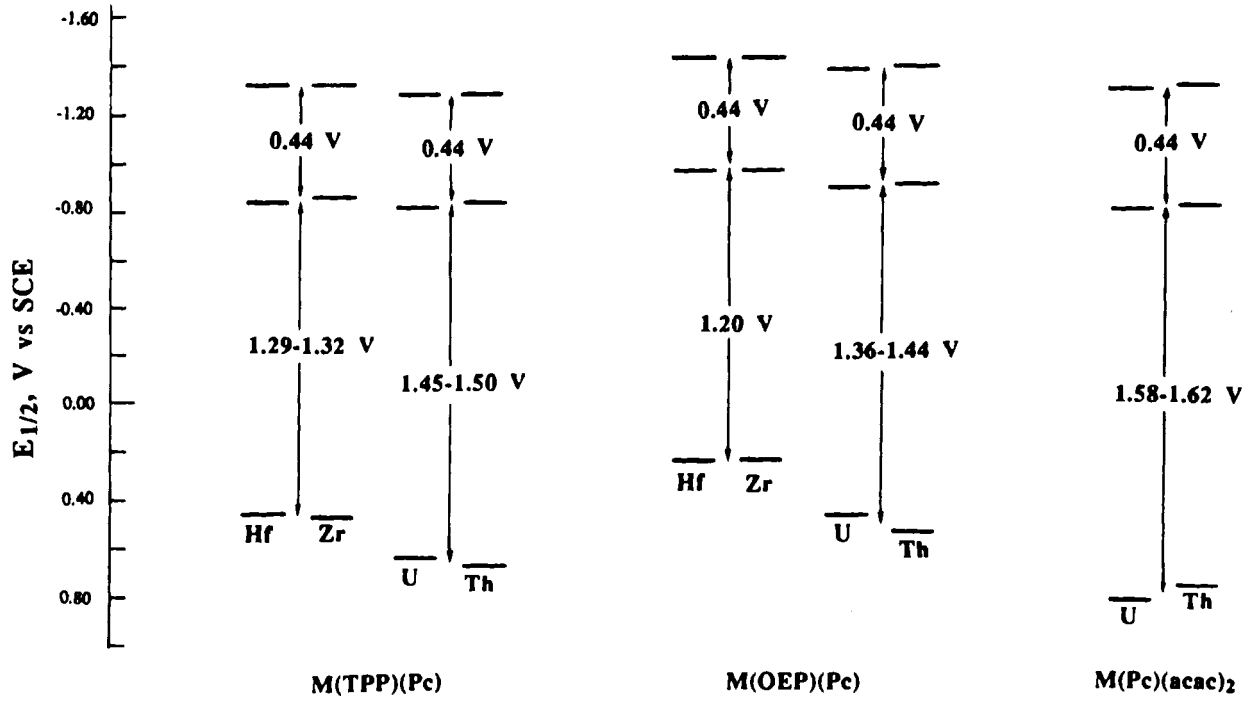

Figure 7. Comparison of potentials for oxidation and reduction of M(P)(Pc) and M(Pc)(acac)$_2$ where P = TPP or OEP and M = Zr, Hf, U, or Th. See Table 5 for actual data.

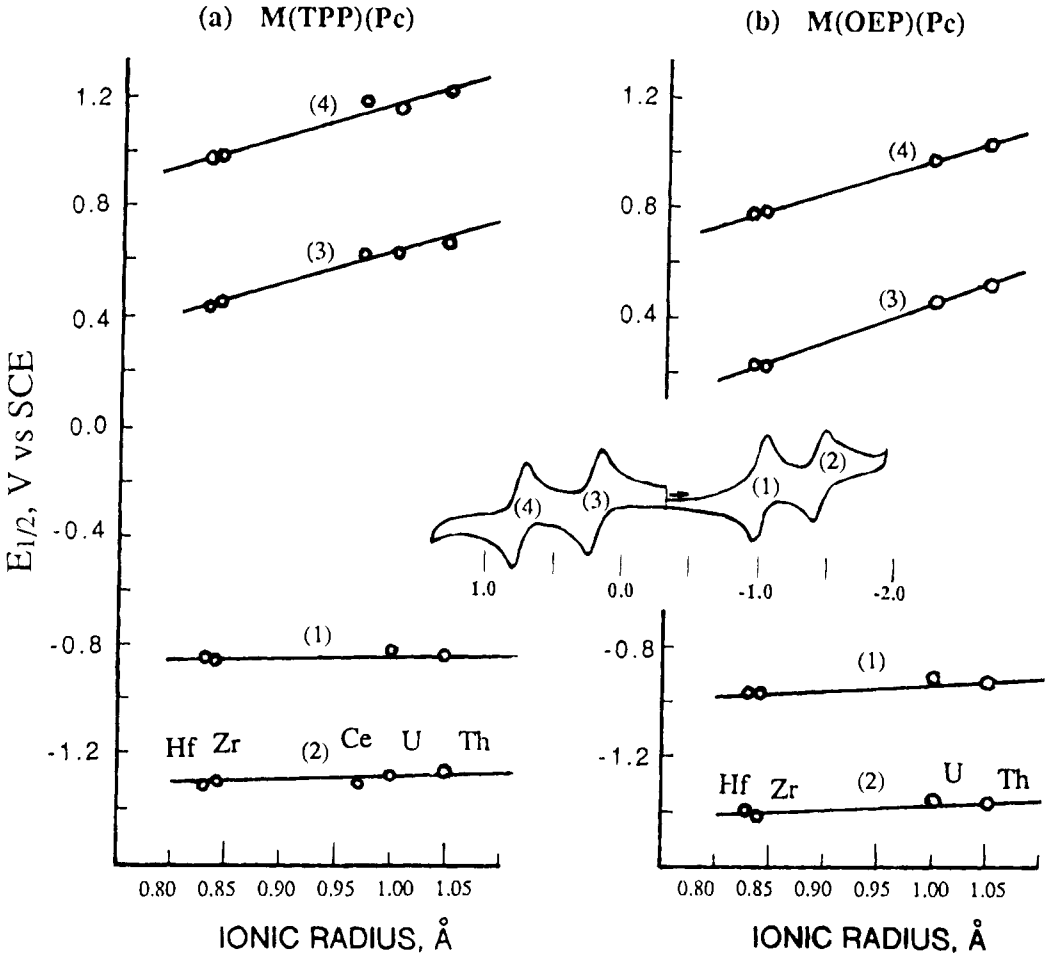

Figure 8. Relationships between redox potentials and ionic radius of the metal ion in (a) M(TPP)(Pc) and (b) M(OEP)(Pc) where M = Hf, Zr, Ce, U, or Th.

upon reduction (see Figure 5 and Table 2) but not upon oxidation, where it remains relatively unchanged (see Figure 4).

Correlations between Spectral and Electrochemical Data and the Site of Electron Transfer. The first two oxidations of M(P)(Pc) involve the stepwise abstraction of two electrons from the HOMO of the double-decker molecule. The first one-electron oxidation of the homoleptic compounds occurs at a half-wave potential of −0.04 V for $Hf(OEP)_2$,[19] +0.54 V for $Hf(TPP)_2$,[19] and +0.48 V for $Hf(Pc)_2$.[5] The similar half-wave potentials for the first oxidation of $Hf(TPP)_2$ and $Hf(Pc)_2$ suggests that one might expect an equal contribution from the TPP and Pc macrocycles in formation of the Hf(TPP)(Pc) HOMO. In constrast, the large difference in potentials between the $E_{1/2}$ for first oxidation of $Hf(OEP)_2$ and that for the first oxidation of $Hf(Pc)_2$ suggests that the abstraction of an electron from M(OEP)(Pc) involves mainly the OEP macrocycle. It also indicates that the HOMO of M(OEP)(Pc) has more OEP than Pc character. Indeed, in the case of M(TPP)(Pc), the two stepwise oxidations seem to affect both the TPP and Pc ring UV absorptions, while changes in the UV−vis spectrum upon oxidation of M(OEP)(Pc) seem to involve mainly the OEP and not the Pc band (see Figure 4).

Despite the large difference in potentials between $E_{1/2}$ values for the first oxidation of M(OEP)(Pc) and the first oxidation of M(TPP)(Pc), there is no large difference in the $E_{1/2}$ values for reduction of these two types of compounds. The UV−vis spectra upon reduction also seem to reflect changes only in the Pc absorptions (see Figures 4 and 5). Both of these results suggest that the reduction of M(P)(Pc) occurs largely at the Pc ring and that the LUMO of the double-decker molecule can be represented mainly by the LUMO of the Pc macrocycle. Indeed, the first reduction of $M(P)_2$ (where M = Zr, Hf, U, and Th) occurs at potentials between −1.3 and −1.6 V,[19,30] while the first reduction of the related $M(Pc)_2$ species occurs at potentials close to −0.6 V.[30] Thus, no significant interaction is expected to occur between the porphyrin and phthalocyanine rings of the electroreduced complexes.

Additional evidence for the site of electron transfer may be obtained from a plot of the UV absorption band energies assigned to the porphyrin or phthalocyanine macrocycle and half-wave potentials for the first oxidation or first reduction of the compound under the same solution conditions (Figure 6). The energy of the porphyrin UV band correlates well with $E_{1/2}$ for the first oxidation of each examined compound (see Figure 6a). However, there are no correlations between $E_{1/2}$ for oxidation and the energy of the phthalocyanine UV band of the same eight derivatives (Figure 6b), thus further indicating that the phthalocyanine ring is not the main site of electron abstraction in the one-electron oxidation process.

All of the reductions occur over a relatively narrow potential range which also corresponds to a narrow range of the Pc absorption band energies (Figure 6b). Finally, no correlation is seen between the energy of the porphyrin UV band and the $E_{1/2}$ for reduction of the eight compounds (Figure 6a), thus suggesting that the first oxidation of M(P)(Pc) involves mainly the porphyrin macrocycle while the first reduction of the same compounds involves primarily the phthalocyanine ring.

A comparison of half-wave potentials for the first reduction and first oxidation of M(P)(Pc) also reveals another surprising

feature. The oxidation potentials strongly depend on both the ionic radius and type of porphyrin ring, but the reduction potentials are almost independent of the metal ionic radius and type of porphyrin ring (see Figure 7). Moreover, the first reduction potentials (-0.90 ± 0.08 V) are very close to the first reduction potential of the related monophthalocyanine derivatives (around -0.85 V)[45] and very far away from the reduction potentials of corresponding U and Th monoporphyrins (~ -1.56 V for $M(OEP)L_2$).[46] The difference between the first and second reductions of the M(P)(Pc) derivatives is constant ($\Delta E_{1/2} = 0.44$ V), suggesting the same site of reduction for all of the compounds. Although the reduction potentials are virtually independent of the metal ionic radii, the oxidation becomes easier with decreasing ionic radius of the metal (see Figure 7). The HOMO−LUMO gap (difference between $E_{1/2}$ values for the first oxidation and the first reduction) is expected to decrease with decreasing distance between the two macrocycles (*i.e.*, with decreasing ionic radius of the metal). This is the case as seen in Figure 8, which also includes data from the literature on the two oxidations and single ring centered reduction of Ce(TPP)(Pc).[33,47] As seen in this figure, the effect on the HOMO−LUMO gap arises from the change in oxidation potential, *i.e;*, the energy of the HOMO, mainly typical of a porphyrin orbital, increases when the ring−ring distance is decreasing. The energy of the LUMO, characteristic of a phthalocyanine orbital, remains relatively constant.

Acknowledgment. The support of The Robert A. Welch Foundation (K.M.K., Grant E-680), the Centre National de la Recherche Scientifique, the National Science Foundation (K.M.K., Grant CHE-8822881), and NATO (Grant 0168/87) is gratefully acknowledged. One of the authors (V.A.A.) is also thankful to the Electrochemical Society for an Energy Research Summer Fellowship Award.

IC941054A

(45) Guilard, R.; Dormond, A.; Belkalem, M.; Anderson, J. E.; Liu, Y. H.; Kadish, K. M. *Inorg. Chem.* **1987**, *26*, 1410−1414.

(46) Kadish, K. M.; Liu, Y. H.; Anderson, J. E.; Dormond, A.; Belkalem, M.; Guilard, R. *Inorg. Chim. Acta* **1989**, *163*, 201−205.

(47) The electrochemical behavior of Ce(TPP)(Pc) differs from those of the other investigated double-decker compounds with tetravalent central metals in that the first reduction, which occurs at $E_{1/2} = -0.05$ V vs SCE in CH_2Cl_2,[33] is a metal-centered Ce(IV)/Ce(III) process rather than a reduction at the ring. Therefore, the potential for this reaction is not shown in Figure 8 which only involves $E_{1/2}$ values for ring-centered electrode reactions. Surprisingly, however, the following reduction of $[Ce^{III}(TPP)(Pc)]^-$, which is ring centered, fits the correlation obtained for ring-centered reductions of the other electrogenerated $[M^{IV}(TPP)(Pc)]^-$ complexes with electroinactive central metal ions. This suggests that the overall charge is more important than the actual site of electron transfer.